

## Electrochemical Impedance Spectroscopy as a Method of Differential Characterization of Electrical Behavior of Self-assembled TiO<sub>2</sub> NTS

M. Pereyra <sup>a\*</sup>, E. Méndez <sup>b</sup>, E. A. Dalchiele <sup>c</sup>

<sup>a\*</sup> Unidad de Bioquímica Analítica, Facultad de Ciencias, Universidad de la República, Montevideo Uruguay

<sup>b</sup> Laboratorio de Biomateriales, Facultad de Ciencias, Universidad de la República, Montevideo, Uruguay

<sup>c</sup> Instituto de Física, Facultad de Ingeniería, Universidad de la República, Montevideo, Uruguay.

\*Corresponding author, E-mail: mpereyra.perez@fcien.edu.uy, phone: (+598) 2525 0901 int. 1302.

### ABSTRACT

Nanotube (NTs) arrays of TiO<sub>2</sub> have received great attention in various areas, such as gas-sensing, photocatalysis, solar energy conversion, and orthopedic implantation. Therefore, particular attempts are carried out to fabricate vertically oriented TiO<sub>2</sub> nanotube arrays by electrochemical anodization in order to improve its properties to meet the practical application requirements. In the present work, the semiconductor behavior of self-organized vertically oriented TiO<sub>2</sub> nanotube fabricated by a controlled corrosion process of electrochemical anodization of titanium foil using a simple method of glycerol based electrolyte (containing 0.27 mol/L NH<sub>4</sub>F and H<sub>2</sub>O in volumetric ratio 1:1) were studied by Electrochemical Impedance Spectroscopy (EIS). Ordered high-aspect-ratio TiO<sub>2</sub> nanotube arrays with an inner tube diameter of ca. 45 nm in average and a tube height of 1 μm were identified by scanning microscopy and atomic force microscopy. TiO<sub>2</sub> NTs semiconductor behavior was compared to a smooth titanium sheet with a spontaneous passivating TiO<sub>2</sub> coating. The results showed that it is possible to represent the interface Ti/TiO<sub>2</sub> electrical behavior as well as surface and the base of the nanotube.

**Keywords:** Electrochemical Anodization, Nanotubes, Titanium dioxide, Electrochemical Impedance Spectroscopy.

### Espectroscopía de Impedancia Electroquímica como Método para la Caracterización diferencial del comportamiento eléctrico de Nanotubos de TiO<sub>2</sub> Autoensamblados

### RESUMEN

Las superficies de nanotubos de TiO<sub>2</sub> ha despertado un gran interés en varias áreas como sensor de gas, conversión de energía solar e implantes ortopédicos. En ese sentido, diferentes iniciativas se han llevado a cabo para la fabricación de nanotubos de TiO<sub>2</sub> orientados verticalmente por anodización electroquímica, con el objetivo de mejorar sus propiedades para alcanzar los requerimientos en aplicaciones prácticas. Si bien la síntesis de nanotubos de TiO<sub>2</sub> por diferentes métodos está ampliamente reportada, las propiedades semiconductoras de los nanotubos siguen siendo un tema de estudio. En el presente trabajo, se estudia el comportamiento semiconductor de una capa de Ti recubierta de nanotubos de TiO<sub>2</sub> orientados verticalmente, sintetizados por anodización electroquímica en una solución a base de glicerol que contiene 0.27 mol/L de NH<sub>4</sub>F en glicerol/agua (1:1 v/v), por el método de Espectroscopía de Impedancia Electroquímica. Se obtuvieron nanotubos de TiO<sub>2</sub> de alta relación de aspecto con un diámetro interno de aproximadamente 45 nm y una altura de 1 μm, identificados por microscopía de barrido y microscopía de fuerza atómica. El comportamiento semiconductor de los nanotubos de TiO<sub>2</sub> fueron comparados con una placa de titanio con capa de TiO<sub>2</sub> pasivante en su superficie generada espontáneamente. Los resultados mostraron que es posible representar el comportamiento eléctrico de la interface Ti/TiO<sub>2</sub>, así como de la superficie y de la base de los nanotubos.

**Palabras claves:** Anodización Electroquímica, Nanotubos, Dióxido de Titanio, Espectroscopía de Impedancia Electroquímica.

### INTRODUCTION

The synthesis of NTs has a great interest in the scientific scope due to the high relation that presents as far as surface-volume and the new properties due to the size. In

particular, the NTs of titanium dioxide have demonstrated several applications in solar cells [1] and biomaterials [2]. A high resistance to corrosion, suitable mechanical properties, and excellent biocompatibility makes one of

the materials of greater application in dental and bony implants [3]. Also, the geometry of vertical growth from the substrate makes them excellent electron percolation pathways for charge transfer between interfaces and offers them improved properties for applications in photocatalysis [4] and hydrogen sensors [5]. Research in new materials for implants and energy storage are a great opportunity for developing countries to lower cost in medicine and the industrial manufacturing. Being able to develop their own products has an important economic and social impact.

In 1999, Zwilling and coworkers reported on anodization of Ti and Ti alloys in electrolytes containing hydrofluoric acid (HF) [6]. Since then, the anodization of Ti has been used to convert the surface of this substrate into highly ordered nanotube. Through anodic oxidation a self-organized process take place [7-9] using a set of specific conditions including optimized potential, temperature and electrolyte compositions [10]. Although the synthesis of TiO<sub>2</sub> NTs by different methods is widely reported [11], the semiconductor properties of NTs are still a subject of study.

Materials impedance measurements is a very promising characterization method because it provides information about the interface behavior between the material surface and the electrolyte solution surrounding [12, 13]. It also can be used as an experimental model to know how the surface modification could interact with simulated biological environment [14-16].

In the present work, the semiconductor behavior of a Ti layer coated with TiO<sub>2</sub> NTs obtained by anodization in a 0.27 mol/L NH<sub>4</sub>F and glycerol/water 1:1 v/v solution is studied by Electrochemical Impedance Spectroscopy (EIS) and compared to the behavior of a titanium sheet with spontaneous formation of a passivating layer of TiO<sub>2</sub>. Scanning Electron Microscopy (SEM) and Atomic Force Microscopy (AFM) techniques allowed to identify the morphology and topographic distribution of the NTs.

## MATERIALS AND METHODS

The samples Ti foils (99.96 % purity, Goodfellow, England) with a thickness of 0.1 mm cut into pieces of 0.80 cm × 2.5 cm were used in all experiments. The samples were degreased prior to anodization by sonicating successively in acetone, isopropanol, and methanol, for 15 min and rinsed with deionized water (DI). Anodization was carried out according to previously published protocol [17]. The electrochemical setup consisted of DC power supply from 0 - 30 V connected to computer and a conventional two-electrode cell, a Ti foils (0.8 cm × 2.5 cm) was used as a working electrode and a Ti sheet (2.5 cm × 2.5 cm) as a counter-electrode. The samples were pressed with a screw to a support leaving a geometric area of 0.8 cm<sup>2</sup> exposed to the electrolyte. A solution containing 0.27 mol/L NH<sub>4</sub>F consisting of a mixture of DI water and glycerol (1,2,3-propanetriol) prepared in a volumetric ratio 1:1 was used. All electrolytes were prepared from reagent grade chemicals and DI water. TiO<sub>2</sub> nanostructures were grown by potentiostatic anodization at 20 V. A potential ramp ranging from 0 V to 20 V with a ramp rate of 2.5 Vs<sup>-1</sup> was applied followed by holding the potential constant for 3.5 hs. After anodization, the samples were rinsed in DI water, sonicating in 0.1 mol/L HCl for 30 s and dried by warm air. To transform amorphous titania into anatase, the samples were annealed at 550°C for 3 h in air in an oven.

### *Surface characterization*

The morphology and structure of the anodized titania NTs were studied by scanning electron microscopy (SEM Joel 5900 low vacuum.). SEM cross-sectional observations and Energy-dispersive X-ray spectroscopy (EDS) were carried out on mechanically cut samples. Powder X-ray diffraction (XRD) patterns of the TiO<sub>2</sub> NTs were recorded with a PHILIPS PW3710 diffractometer using CuK $\alpha$  radiation. AFM images (Digital Instruments Nanoscope III) were taken in University of Valparaíso, Chile.

The impedance measurements were carried out in a Voltalab potentiostat model PGZ301, Radiometer (Switzerland) in an aqueous solution of 1 M Na<sub>2</sub>SO<sub>4</sub>, using a Platinum plate as a counter electrode and a saturated calomel electrode (SCE) as a reference. A potential sweep was performed from 0 mV to -1300 mV and a frequency sweep from 10 mHz to 10 kHz, with a signal amplitude of 10 mV. The measurements were carried out after 2 min of each potential, until reaching equilibrium. All potentials in the text are referred to the saturated calomel electrode (SCE). The circuit elements were fitted by Chi-square parameter ( $\chi^2$ ).

## RESULTS AND DISCUSSION

Electrochemical anodization can be interpreted as a controlled corrosion process of the metal in which the oxide layer is formed on the surface. When the Ti foils are anodized, the surface properties change remarkably with the anodization time. In the initial step, a compact oxide barrier layer is formed on the electrolyte-metal interface, which leads the current to decrease sharply due to the low conductivity of metal oxide in all samples [18]. After a local thinning of the oxide barrier layer happens, due to the effect of the gradually enhanced electric-field assistant dissolution of titania, and random growing pore start. Then the current density keeps relatively stable value since it reaches the maximum dissolution rate of titania at the nanotube bottom. By further anodization, a self-organized nanotube layer is being fully evolved [19]. After samples were annealed at 550 °C for 3 h, amorphous NTs converts into crystalline anatase and rutile phase.

### *Morphological and physicochemical characterization*

Figure 1a and 1b shows SEM images of the samples anodized at 20 V in 0.27 mol/L NH<sub>4</sub>F in deionized water and glycerol in a volumetric ratio 1:1. The images are top as the image shows, self-organized TiO<sub>2</sub> NTs 1 μm long layer vertically oriented were synthesized.

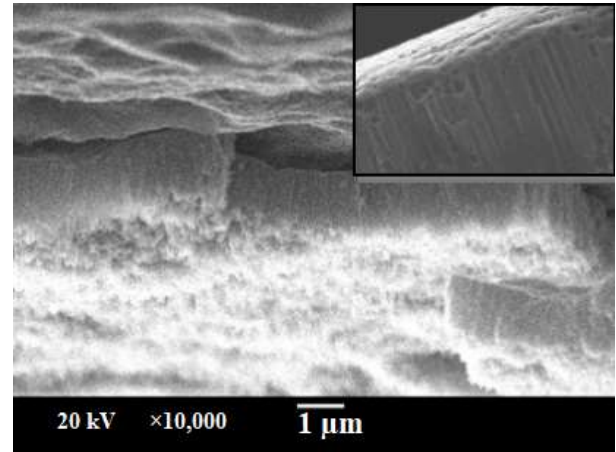


**Fig. 1a.** SEM images of cross-section TiO<sub>2</sub> layer 1 μm long.

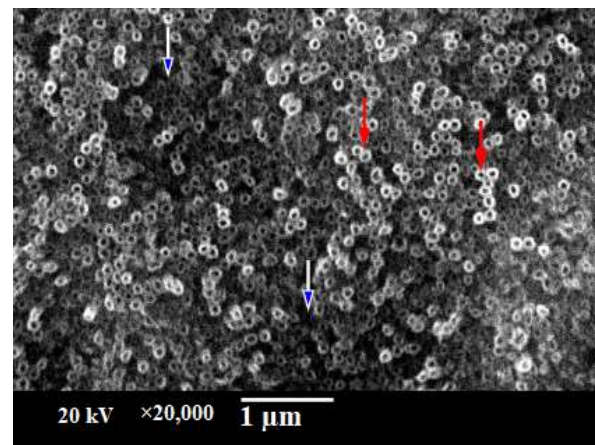


**Fig. 1b.** SEM images top-view shows different width circular rings and random height distribution of the high aspect ratio nanotubes (blue arrows: lower; red arrows: higher)

Figure 2a and 2b represent the NTs topographical distribution and nanotube inner height from a surface section of the sample. The AFM microscopy allowed to identified the inner height of the NTs that is 100 nm in average. That means the nanotube is not hollow across the entire width of the coated layer. The topographic profiles showed the high degree of compaction of the NTs obtained. On the other hand, they confirm that between the NTs, there was no remnant material of the original surface, but that it was undermined until it reached the base of the nanotube.

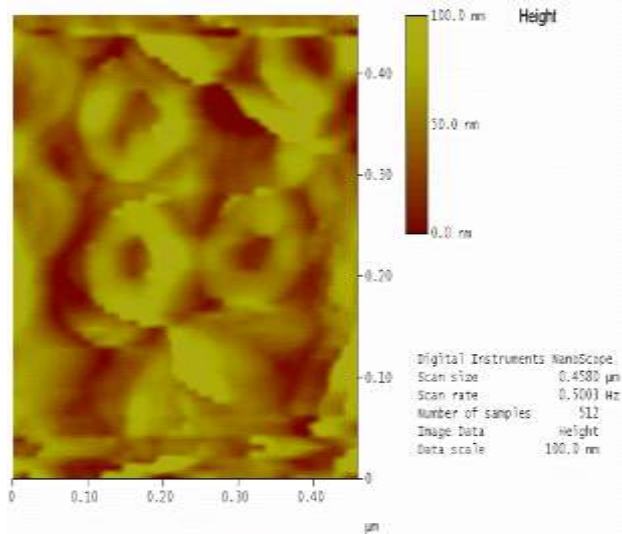
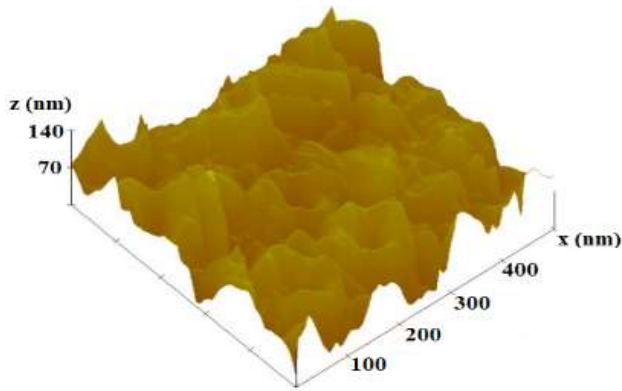


**Fig. 2b.** AFM images of (a) the nanotube distribution on the Ti surface and (b) the height of the TiO<sub>2</sub> NTs.

The dimensions for the internal and external diameters are within the range of values obtained by SEM: 49 nm for the x-axis and 54 nm for the y-axis, which allows the NTs to be described as slightly distorted cylinders (Fig. 3).

The electron dispersion spectroscopy (EDS) allows obtaining information on the chemical composition of selected regions of the surface through SEM microscopy. When the nanotube coating was analyzed, it was possible to identify differential chemical composition of the base and walls of the TiO<sub>2</sub> NTs (Figure 4). While the base of the nanotube is mainly characterized by titanium, TiO<sub>2</sub> predominates on the walls.

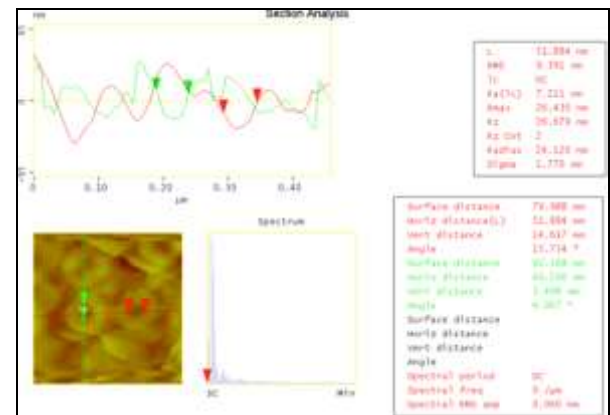
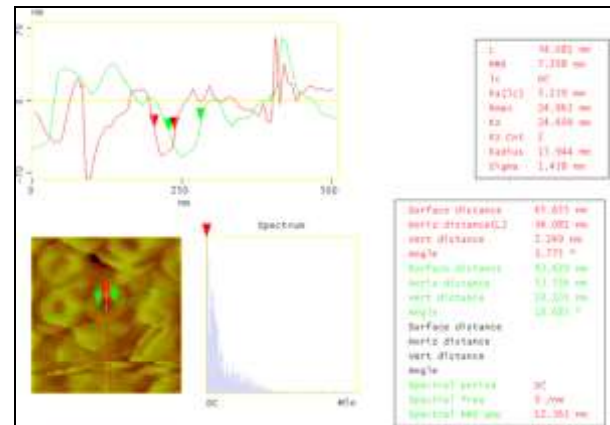


**Fig. 3.** AFM images representing the topographic analysis of titanium nanotube surface sections.

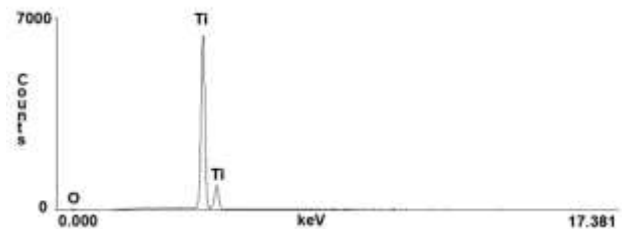


**Fig. 4a.** Spectrum of X-ray dispersion (EDS) for the electrons of the k level of a section of the base of the nanotubes.

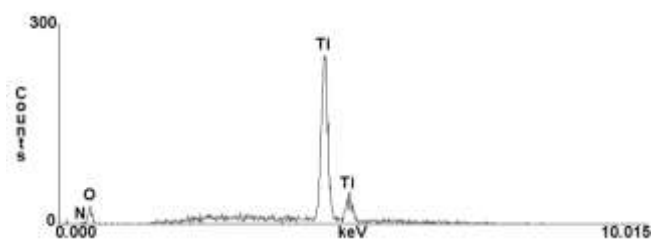


**Fig. 4b.** Spectrum of X-ray dispersion (EDS) for the electrons of the k level of a section of the walls of the nanotubes.

In Table I differential chemical composition in terms of atoms and weight percentage are showed.

**Table I.** EDS chemical composition in terms of atoms and weight percentage

TiO <sub>2</sub> NTs	Element	atoms %	wt % element	Error wt %
Base	O-K	4.29	1.47	+/- 0.16
	Ti-K	95.71	98.53	+/- 0.45
Wall	O-K	40.89	19.25	+/-1.19
	Ti-K	56.53	79.69	+/- 1.43
	N-k	2.58	1.06	+/-0.46

The walls of the NTs showed signals corresponding to the main presence of Ti and O, along with other minor elements, in Ti:O atomic ratios of 56:41 in percentage. The evaluation of the base of the titanium NTs resulted in an EDS profile different from that obtained for the walls. In this case, the almost exclusive presence of titanium is observed. It was evidenced, at a qualitative level, that the

chemical composition of the walls and the base is different, and that the process of formation of the NTs involves oxidation on the titanium surface.

It should be noted that the EDS technique is not good at quantitative evaluation of lighter elements. Therefore, the results obtained must be evaluated only qualitatively.

#### *Electrochemical behavior*

Electrochemical impedance spectroscopy studies the response of the system to a periodic AC disturbance of small amplitude, sweeping a wide spectrum of frequencies. The impedance spectra obtained were adjusted to different circuits containing combinations of resistors (R), capacitors (C), constant phase elements (CPE) and Warburg elements (W). The choice of the best circuit was based on the adjustment parameter  $\chi^2$ . The impedance of each of these elements, in their real (Z') and imaginary (Z'') components are summarized in Table II.

**Table II.** Summary of impedance elements.

Circuit Element	Real and Imaginary Contribution			Parameters of Eq.
Resistor: R	$Z = R$	$Z' = R$	$Z'' = 0$	
Capacitor: C	$Z = \frac{1}{\omega c}$	$Z = 0$	$Z = \frac{1}{i\omega c}$	
Constant Phase Elements: CPE	$Z = \frac{1}{Y} (i\omega)^n$			CPE-T, CPE-P
Warburg Diffusion Element: W	W <sub>s</sub> :	$Z = \frac{1}{Y} \sqrt{i\omega}$		Parameters: Ws-R, Ws-T, Ws-P  Parameters: Wo-R, Wo-T, Wo-P
	W <sub>o</sub> :	$Z = \frac{1}{Y} \sqrt{i\omega} \coth(B\sqrt{i\omega})$		
	W <sub>T</sub> :	$Z = \frac{1}{Y} \sqrt{i\omega} \tanh(B\sqrt{i\omega})$		

Figure 5 shows the cyclic voltammetry of the Ti sheet coated with passivating oxide and with TiO<sub>2</sub> NTs to determine the electrochemical behavior of the surfaces in the range of potentials in which the impedance measurements were made. In the range of potential

between 0 V and -1.3 V, the surface of NTs shows a significant increase in current density, both in the anodic and cathodic current, given by the surface increase due to the NTs. This is because the current densities were calculated based on the geometric area of the electrodes.

For potentials below -0.5 V, the current density increases progressively, and this increase becomes significant below -0.9 V. In this region, the processes prior to the hydrogen evolution reaction (HER) begin to occur.

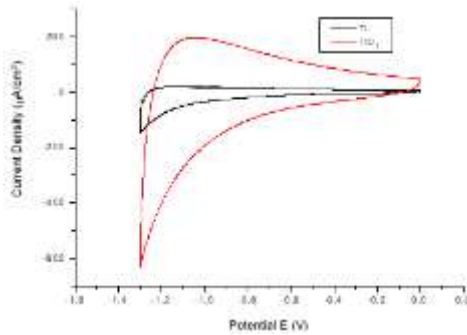


**Fig. 5.** Cyclic voltammetry of Ti sheet coated with TiO<sub>2</sub> nanotubes (red line) and smooth Ti sheet (black line).

Figure 6 shows the capacitive behavior of the passivating oxide layer that covers the Ti surface in which a gradual behavior is observed.

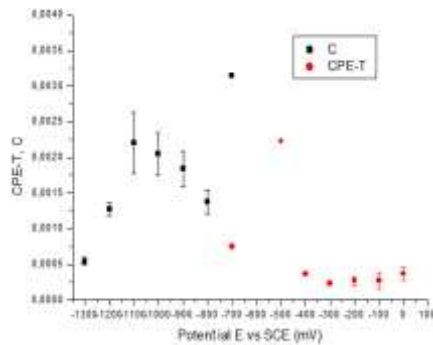


**Fig. 6.** Capacitance of the Ti sheet. From 0 to -0.700 mV it has a CPE-T capacitor behavior, from -800 to -1300 mV it shows a pure C capacitor behavior. Between -500 mV and -700 mV is the transition zone.

In the range from 0 to -700 mV, the capacitor representing the metal surface behaves like a CPE due to the partial coating of the surface with a passivating layer of titanium oxide, which gives rise to surface heterogeneities, and suggests the existence of roughness on the metal during the oxidation process. From this point, and as the potential decreases towards more negative values, the system enters the hydrogen evolution zone in which the oxide surface would be removed, leaving the

metal exposed. From this value the metal has a pure capacitor behavior. For the lowest potentials (below -1200 mV) a decrease in capacitance related to titanium hydride formation processes is observed. Between -500 mV and -700 mV is the transition zone which cannot be adjusted by either of the two proposed circuits.

Two circuits were adjusted in order to represent the aforementioned behavior (Fig. 7). The circuit represents the partially oxidized Ti surface in which the elements of the solution interact with both the oxidized and the exposed surface, therefore the system is represented with two R-CPE circuits in series. From -700 mV and towards more negative values, the metal surface is uncovered and behaves like a pure capacitor.

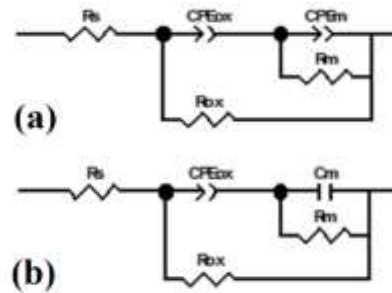


**Fig. 7.** Equivalent circuits used to describe the interface formed by a smooth titanium sheet in solution. (A) potential range between 0 and -700 mV, (B) potential range between -800 and -1300 mV.

The TiO<sub>2</sub> / electrolyte interface has been modeled by a simple equivalent circuit where the resistance of the solution is in series with a constant phase element CPE [20]. Contrary to what happens with the smooth titanium surface, when it is covered by titanium oxide NTs, the Nyquist diagram shows a contribution at low frequencies corresponding to a Warburg impedance. In the Nyquist graph (Fig. 8), a semicircle is observed at the beginning that can be associated with a resistive and capacitive process.



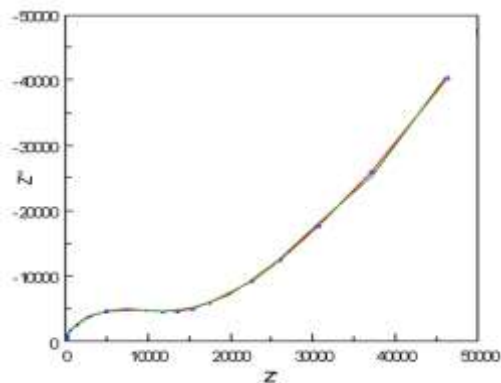


**Fig. 8.** Nyquist plot for the TiO<sub>2</sub> NTs with the corresponding fit according to the proposed circuit model.

After this area, a growth is observed in a straight line with a certain angle with respect to the  $Z'$  axis, which corresponds to diffusion processes. For this reason, to describe the behavior of the nanotube layer as well as the underneath Ti plate for potentials between 0 and -700 mV, a branch including a CPE in parallel with a combination of a resistive element in series with a Warburg ( $W_s$ ) element was added (Fig. 9).

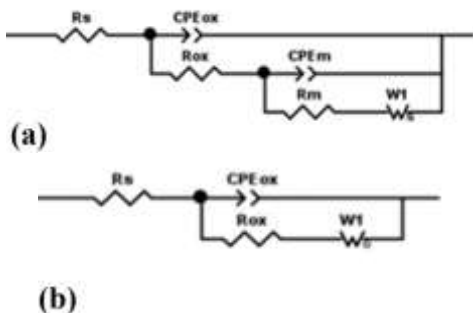


**Fig. 9.** Equivalent circuits modeling the interface of the titanium surface covered by TiO<sub>2</sub> nanotubes. Potential range between (a) 0 and -700mV, (b) -800 and -1300 mV. For lower potentials, it was no longer possible to adjust with the previous model, therefore, a Warburg diffusional element,  $W_s$ , was added to the R-CPE circuit. This model allows the values to be adjusted with a relative error for the real and imaginary part of the impedance of less than 1% for the entire frequency range.  $R_{ox}$  and  $CPE_{ox}$  are associated with the resistance to charge transfer and the capacitance of the nanotube layer, respectively, and the  $W_s$  element corresponds to diffusional processes that

would be occurring on the surface without a defined mechanism.

In Figure 10, the capacitance of the TiO<sub>2</sub> NTs is represented where an increase is observed for more negative values of potential. As the system reaches the hydrogen evolution zone, the nanotube layer becomes more polarizable, possibly due to the diffusion processes observed from -700 mV.

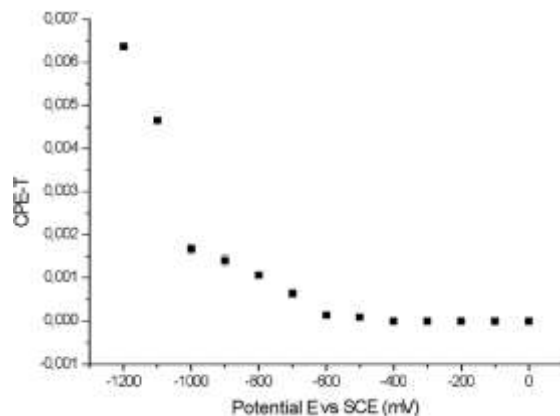


**Fig. 10.** Graph corresponding to the surface capacitance of TiO<sub>2</sub> NTs.

The difference between the circuits used in the smooth titanium sheet and the NTs, in addition to the presence of a Warburg element, is it because part of the titanium surface below the NTs is exposed to the electrolyte, either by the existence of regions where the density of NTs is lower, or because the NTs base is titanium. The adjustment of this circuit to the experimental data confirms the existence of a metallic titanium base below the NTs.

**CONCLUSIONS**

The presence of titanium NTs can be detected by Electrochemical Impedance Spectroscopy showing a differential behavior regarding the unmodified metal surface. From the parameters of the circuits, it is possible to obtain the electrical characteristics of the interface Ti/TiO<sub>2</sub>, fundamental information for the use of surfaces modified with TiO<sub>2</sub> NTs in solar cells or as a base material

for the electrochemical synthesis of coatings such as hydroxyapatite. Microscopy techniques allowed not only to determine the topography of the nanotube coating as well as their morphology, but also complemented the information obtained by EIS.

#### ACKNOWLEDGEMENT

This work was funded by PEDECIBA (Programa para el Desarrollo de Ciencias Básicas) and SNB-ANII (Sistema Nacional de Becas). Special thanks to Microscopy Laboratory of the University of Valparaíso, Chile for the AFM images and to Ph.D. Alejandro Marquez (R.I.P.) for his excellent disposition in collaborating with the investigation through SEM micrographs (Laboratorio de Microscopía de Barrido, Facultad de Ciencias, Uruguay).

#### CONFLICTS OF INTEREST

The authors declare no conflict of interest.

#### REFERENCES

- [1] Bai Y., Mora-Seró I., De Angelis F., Bisquert J., Wang P. (2014) “Titanium dioxide nanomaterials for photovoltaic applications” *Chem. Rev.* 114(19):10095–10130.
- [2] Bhatia S.K. (2010) “*Biomaterials for clinical applications*” New York, Springer. DOI: 10.1007/978-1-4419-6920-0.
- [3] Mazare A., Totea G., Burnei C., Schmuki P., Demetrescu I., Ionita D. (2016) “Corrosion, antibacterial activity and haemocompatibility of TiO<sub>2</sub> NTs as a function of their annealing temperatura” *Corros. Sci.* 103:215-222. DOI: 10.1016/j.corsci.2015.11.021.
- [4] Hosseinpour P. M., Panaitescu E., Heiman D., Menon L., Lewis L. H. (2013) “Toward tailored functionality of titania nanotube arrays: Interpretation of the magnetic-structural correlations” *J. Mater. Res.* 28(10):1304-1310. DOI: 10.1557/jmr.2013.94.

- [5] Ratan S., Kumar C., Kumar A., Jarwal D. K., Mishra A. K., Jit S. (2018) “Fabrication and Characterization of Titanium Dioxide Based Pd/TiO<sub>2</sub>/Si MOS Sensor for Hydrogen Gas” *IEEE Sens. J.* 18(10):3952-3959. DOI: 10.1109/jsen.2018.2819805.
- [6] Zwilling V., Darque- Cerretti E., Boutry-Forveille A., David D., Perrin M.Y., Aucouturier M. (1999) “Structure and physicochemistry of anodic oxide films on titanium and TA6V alloy” *Surf. Interface Anal.* 27:629-637. DOI: 10.1002/(SICI)1096-9918(199907)27:7<629::AID-SIA551>3.0.CO;2-0.
- [7] Gong D., Grimes C.A., Varghese O.K., Hu W., Singh R.S., Chen Z., Dickey E.C. (2001) “Titanium oxide nanotube arrays prepared by anodic oxidation” *J. Mater. Res.* 16(12):3331-3334. DOI: 10.1557/JMR.2001.0457.
- [8] Macak J.M., Schmuki P. (2006) “Anodic growth of self-organized anodic TiO<sub>2</sub> NTs in viscous electrolytes” *Electrochim. Acta* 52:1258-1264. DOI: 10.1016/J.ELECTACTA.2006.07.021.
- [9] Prakasam H. E., Shankar K., Paulose M., Varghese O. K., Grimes C. A. (2007) “A new benchmark for TiO<sub>2</sub> nanotube array growth by anodization” *J. Phys. Chem. C* 111:7235-7241. DOI: 10.1021/jp070273h.
- [10] Kulkarni M., Mazare A., Schmuki P., Iglıc A. (2016) “Influence of anodization parameters on morphology of TiO<sub>2</sub> nanostructured surfaces” *Adv. Mater. Lett.* 7(1):23-28. DOI: 10.5185/amlett.2016.615.
- [11] Awad N. K., Edwards S. L., Morsi Y. S. (2017) “A review of TiO<sub>2</sub> NTs on Ti metal: Electrochemical synthesis, functionalization and potential use as bone implants” *Mater. Sci. Eng. C* 76:1401–1412. DOI: 10.1016/j.msec.2017.02.150.
- [12] Gharbi O., Ngo K., Turmine M., Vivier V. (2020) “Local electrochemical impedance spectroscopy: A window into heterogeneous interfaces” *Curr. Opi. Electrochem.* 20:1-7. DOI: 10.1016/j.coelec.2020.01.012.



- [13] Liang Y., Gao F., Wang L., Lin S. (2021) “In-situ monitoring of polyelectrolytes adsorption kinetics by electrochemical impedance spectroscopy: Application in fabricating nanofiltration membranes via layer-by-layer deposition” *J. Membr. Sci.* 619:118747. DOI: 10.1016/j.memsci.2020.118747.
- [14] DuToit M., Ngaboyamahina E., Wiesner M. (2021) “Pairing electrochemical impedance spectroscopy with conducting membranes for the in situ characterization of membrane fouling” *J. Membr. Sci.* 618:118680. DOI: 10.1016/j.memsci.2020.118680.
- [15] Krukiewicz K. (2020) “Electrochemical impedance spectroscopy as a versatile tool for the characterization of neural tissue: A mini review” *Electrochem. Commun.* 116:106742. DOI: 10.1016/j.elecom.2020.106742.
- [16] Raila T., Ambrulevičius F., Penkauskas T., Jankunec M., Meškauskas T., Vanderah D. J., Valincius G. (2020) “Clusters of protein pores in phospholipid bilayer membranes can be identified and characterized by electrochemical impedance spectroscopy” *Electrochim. Acta* 364:137179. DOI: 10.1016/j.electacta.2020.137179.
- [17] Pereyra M., Méndez E., Dalchiele A. (2011) “Nanotubos de orientación vertical autoensamblados por método electroquímico síntesis y caracterización” *PUENTE* 5(2):45-49. ISSN: 19099051.
- [18] Yu X., Li Y., Wlodarski W., Kandasamy S., Kalantar-zadeh K. (2008) “Fabrication of nanostructured TiO<sub>2</sub> by anodization: A comparison between electrolytes and substrates” *Sens. Actuators B* 130:25-31. DOI: 10.1016/j.snb.2007.07.076.
- [19] Macak J.M., Hildebrand H., Marten-Jahns U., Schmuki P. (2008) “Mechanistic aspect and growth of larger diameter self-organized TiO<sub>2</sub> nanotube” *J. Electroanal. Chem.* 621:254-266. DOI: 10.1016/J.JELECHEM.2008.01.005.
- [20] Zaban A., Meier A., Gregg B. A. (1997) “Electric Potential Distribution and Short-Range Screening in Nanoporous TiO<sub>2</sub> Electrodes” *J. Physc. Chem. B* 101:7985-7990. DOI: 10.1021/jp971857u.